J. Plasma Phys. (2016), *vol.* 82, 515820101
doi:10.1017/S0022377815001476

Study of collisionless high-energy charged particle losses for stellarators in presence of resonant perturbations of the magnetic field

V. V. Nemov[1,2,†], S. V. Kasilov[1,2], W. Kernbichler[2] and V. N. Kalyuzhnyj[1]

[1]Institute of Plasma Physics, National Science Center 'Kharkov Institute of Physics and Technology', Akademicheskaya str. 1, 61108 Kharkov, Ukraine

[2]Institut für Theoretische Physik – Computational Physics, Technische Universität Graz, Fusion@ÖAW, Petersgasse 16, A-8010 Graz, Austria

(Received 28 August 2015; revised 17 December 2015; accepted 17 December 2015)

Using a numerical code based on guiding centre drift equations, collisionless high energy particle losses, and in particular α-particle losses, are studied for a number of stellarator configurations in the presence of magnetic islands caused by resonant perturbations of magnetic surfaces. Standard stellarator configurations, as well as an optimized quasi-helically symmetric stellarator, are used in this study. It is found that the role of islands in collisionless α-particle losses is practically negligible for standard stellarators, however, for optimized stellarators, islands can have a negative impact.

1. Introduction

One feature of stellarator magnetic configurations is the appearance of island magnetic surfaces caused by resonant perturbations of the main magnetic field of the device. In addition, various deviations from nested flux surfaces can be a result of, e.g. inaccuracies of the magnets or an asymmetric arrangement of some individual elements of the magnetic system.

Formation of magnetic islands can lead to an increased particle and heat transport across the magnetic field in long mean-free-path regimes of transport because of a larger step size of diffusion in the island regions. For the collisionless regimes of confinement, which are important for assessment of the general confinement properties of stellarators (Grieger *et al.* 1992) (high energy particle confinement and specifically α-particle confinement, see, e.g. in Lotz *et al.* (1992)) the role of magnetic islands has to be analysed for every specific case, which is done in this paper for a number of specific stellarator magnetic configurations.

In numerical studies of collisionless charged particle losses (in particular, α-particle losses) in stellarators the most consistent approach is realised in codes which perform direct computations of particle losses using guiding centre drift equations to follow charged particle orbits, until such particles are lost. Since the impact of magnetic islands can only be analysed in real space coordinates, the corresponding code of

† Email address for correspondence: nemov@ipp.kharkov.ua

Nemov, Kasilov & Kernbichler (2014) using real space coordinates is employed here, in contrast to analogous codes using magnetic coordinates (see, e.g. Lotz *et al.* 1992).

Here, calculations of the life time of α-particles are performed for U-2M (Uragan-2M (Pavlichenko 1993)) and U-3M (Uragan-3M (Lesnyakov *et al.* 1992)), which represent the 'standard' branch of torsatrons. In addition, the optimized quasi-helically symmetric stellarator (Nührenberg & Zille 1988) (QHS) is also analysed. Sizes and plasma parameters of all configurations are adapted to reactor parameters to allow for computation of α-particle losses.

2. Computational procedure and initial conditions

In the approach of Nemov *et al.* (2014) a sample of 1000 particles (trapped plus passing) is followed with random starting points, as well as random values of pitch angles, on an initial magnetic surface. The guiding centre drift equations are solved within a relevant time interval. Every particle orbit is followed until the particle reaches some limiting surface outside the plasma confinement region. From the general sample of particles, trapped particles give the principal contribution to the collisionless particle losses. All classes of trapped particles are taken into account, i.e. particles trapped in one magnetic field ripple or in several adjacent ones.

Calculations are performed for the life time of 3.5 MeV α-particles in the stellarator magnetic configurations indicated above. They are adapted to reactor plasma parameters choosing $a = 1.6$ m and $B = 5$ T (see Lotz *et al.* (1992), a is the plasma average radius, B is the magnetic field strength).

To accelerate computations, a Lagrange polynomial interpolation of the magnetic field is applied. The influence of an ambipolar radial electric field is not taken into account because it has only a negligible effect on α-particle motion.

Results are presented in plots of the collisionless time evolution of the trapped α-particle fraction. A decrease of this time corresponds to an increase of particle losses.

3. Magnetic configurations of type of U-2M and U-3M

The U-2M device (Pavlichenko 1993) is an $l = 2$ torsatron with 4 helical field periods along the torus. Two different magnetic configurations of U-2M are considered here. For both configurations, the magnetic field parameters are chosen to provide magnetic surfaces which are well centred with respect to the vacuum chamber. For the first configuration, the toroidal magnetic field is chosen in such a way that the rotational transform ι is within $1/3 < \iota < 1/2$ ($k_\varphi = 0.31$, with $k_\varphi = B_{th}/(B_{th} + B_{tt})$ where B_{th} and B_{tt} are the toroidal components of the magnetic field produced by the helical winding and the toroidal field coils, respectively (see, Pavlichenko 1993)). The second configuration ($k_\varphi = 0.295$) has a slightly larger toroidal magnetic field and ι within $0.31 < \iota < 0.383$. For this configuration, the resonant magnetic surfaces with $\iota = 1/3$ are inside the confinement region. For both configurations the magnetic field is calculated using the Biot–Savart law code, where current feeds and detachable joints of the helical winding are taken into account.

Due to the asymmetric arrangement of these elements, the stellarator symmetry of the magnetic field of U-2M is broken and considerable island magnetic surfaces arise, which correspond to $\iota = 1/3$ ($k_\varphi = 0.295$) and $\iota = 2/5$ ($k_\varphi = 0.31$), see figure 1.

The U-3M device (Lesnyakov *et al.* 1992) is an $l = 3$ torsatron with 9 helical field periods along the torus. A peculiarity of its standard configuration is that it is an outward shifted configuration to improve MHD stability. It is stated in Lesnyakov *et al.*

https://doi.org/10.1017/S0022377815001476 Published online by Cambridge University Press

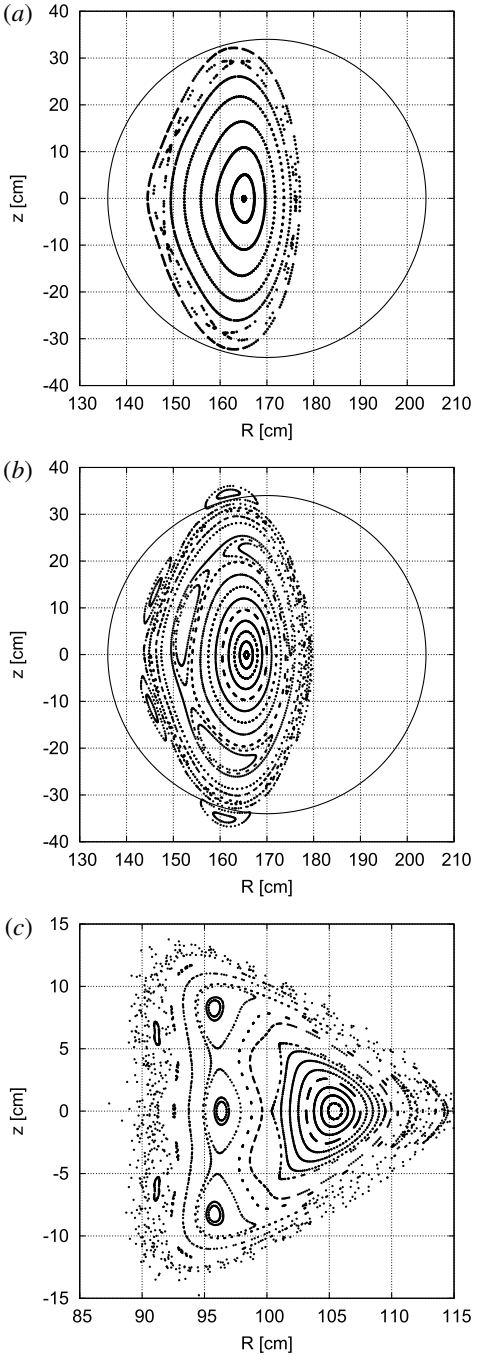

FIGURE 1. Magnetic surfaces for U-2M and U-3M; (*a*) for U-2M, $k_\varphi = 0.31$, island surfaces corresponding to $\iota = 2/5$ are present; (*b*) for U-2M, $k_\varphi = 0.295$, island surfaces corresponding to $\iota = 1/3$ are present; (*c*) for U-3M, island surfaces corresponding to $\iota = 1/4$ are present. A circle with a radius of 34 shows the inner boundary of the vacuum chamber for U-2M.

https://doi.org/10.1017/S0022377815001476 Published online by Cambridge University Press

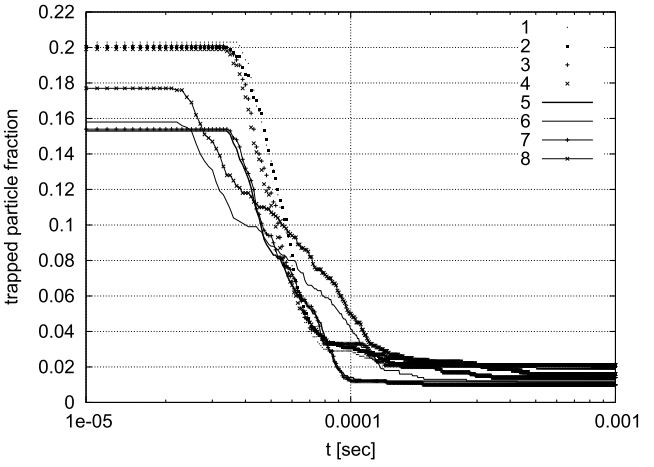

FIGURE 2. Collisionless evolution of the trapped α-particle fractions for the configurations of the U-2M and U-3M types adapted to reactor parameters. 1: for U-2M, $k_\varphi = 0.295$, with islands, 2: for U-2M, $k_\varphi = 0.295$, without islands, 3: for U-2M, $k_\varphi = 0.31$, with islands, 4: for U-2M, $k_\varphi = 0.31$, without islands, 5: for U-3M, $r/a \approx 0.25$, without islands, 6: for U-3M, $r/a \approx 0.5$, without islands, 7: for U-3M, $r/a \approx 0.25$, with islands, 8: for U-3M, $r/a \approx 0.5$, with islands; for U-2M particles are started on the magnetic surfaces corresponding to $A \approx 40$.

(1992) that small errors in the U-3M magnetic system exist. They are equivalent to a small eccentricity in the vertical field coils. The corresponding perturbations of the U-3M magnetic field lead to the appearance of large magnetic islands corresponding to $\iota = 1/4$ inside the confinement region. The magnetic field for the U-3M vacuum configuration is calculated using the helical winding field decomposition into toroidal harmonic functions (with 33 harmonics) and using complete elliptic integrals of the first and second kind for the field of the vertical field coils. Figure 1(*c*) shows the cross-sections of magnetic surfaces and island structures of U-3M.

Computational results for the collisionless time evolution of the trapped α-particle fractions obtained for all three configurations are presented in figure 2. The results relate to particles started on magnetic surfaces corresponding to $A \approx 40$ for U-2M (A is the aspect ratio of the magnetic surface). The limiting surface is the inner surface of the vacuum chamber. For U-3M particles are started on magnetic surfaces corresponding to $r/a \approx 0.25$ and $r/a \approx 0.5$ (r is a mean radius of the magnetic surface). Here, a toroidal surface including the confinement region is considered as the limiting surface.

If current feeds and detachable joints of the helical winding in U-2M, and the eccentricity of the vertical field coils in U-3M, are not taken into account, the corresponding magnetic surfaces become nested regular surfaces. For such magnetic configurations without islands the life time of α-particles is also calculated and those additional results are presented in figure 2.

It follows from the results that there is no noticeable difference for the particle life time in both configurations of U-2M. For the U-3M configuration, the loss time is approximately the same for $r/a = 0.25$ and $r/a = 0.5$. Also, the presence of magnetic islands caused by a violation of the stellarator symmetry in U-2M or a small eccentricity in the vertical field coils in U-3M has no noticeable influence on the life time of α-particles.

https://doi.org/10.1017/S0022377815001476 Published online by Cambridge University Press

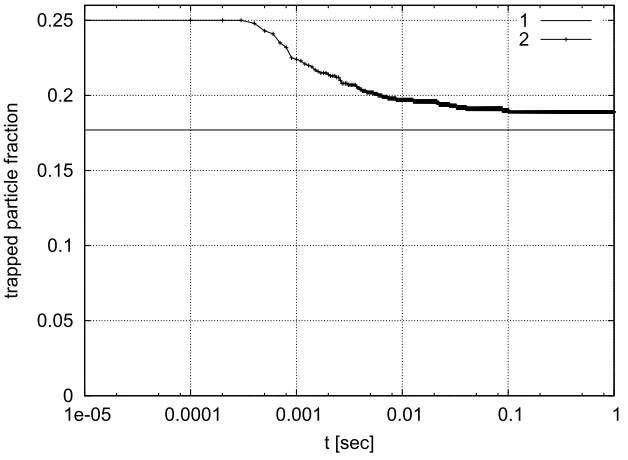

FIGURE 3. Collisionless evolution of the trapped α-particle fractions for the quasi-helically symmetric stellarator adapted to reactor parameters. Particles are started on the magnetic surfaces corresponding to $r/a \approx 0.25$ (1) and $r/a \approx 0.5$ (2) with r being a mean radius of the magnetic surface.

For all three configurations, the approximate α-particle loss time is 10^{-4} s. This is approximately the same value as it was found in Lotz *et al.* (1992) for the standard $l = 2$ stellarator adapted to reactor parameters. This value is unacceptably low for a nuclear fusion reactor and, therefore, the standard stellarators need to be optimized with respect to particle confinement time and transport (see, e.g. Grieger *et al.* 1992).

4. Quasi-helically symmetric stellarator

Quasi-helically symmetric stellarators (QHS stellarators) represent one way to improve the particle and energy confinement in stellarators. In Nührenberg & Zille (1988) the possibility for the existence of quasi-helically symmetric toroidal stellarators has been shown in magnetic coordinates. Calculations of α-particle losses in some quasi-helically symmetric configurations performed in magnetic coordinates in Lotz *et al.* (1992) have demonstrated a very good confinement for particles, which are started in the inner half of the device. A real-space realization of a zero-beta variant of the quasi-helically symmetric configuration (Nührenberg & Zille 1988) (with 6 field periods along the torus) has been considered in Nemov *et al.* (2014) with a magnetic field presented as a decomposition in toroidal harmonic functions containing the associated Legendre functions. The decomposition coefficients of the superposition have been obtained by minimizing the magnetic field component normal to the boundary magnetic surface given by the three-dimensional Variational Moments Equilibrium Code (VMEC) (Hirshman & Betancourt 1991) equilibrium in Nührenberg & Zille (1988) (the Neumann boundary condition at the VMEC boundary).

Computational results for the collisionless time evolution of the trapped α-particle fraction obtained in Nemov *et al.* (2014) for QHS are given in figure 3. The α-particle loss time is essentially larger than in all variants of Uragan. Figure 3 shows that during 1 s trapped particles initiated at $r/a \approx 0.25$ are not lost, however, some fraction of particles initiated at $r/a \approx 0.5$ is lost. Results for $r/a \approx 0.25$ are in good agreement with the results of Lotz *et al.* (1992) using magnetic coordinates, however, results for

https://doi.org/10.1017/S0022377815001476 Published online by Cambridge University Press

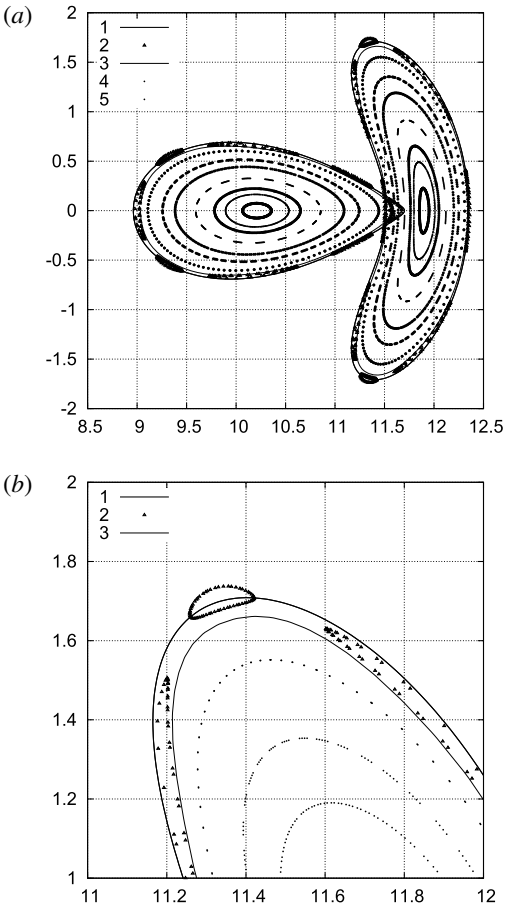

FIGURE 4. Magnetic surface cross-sections of the quasi-helically symmetric stellarator. (*a*) Bean shaped and after a half of the field period; (*b*) with increased scale for magnetic islands. 1: VMEC boundary, 2: island surfaces $\iota = 3/2$, 3: the magnetic surface just inside $\iota = 3/2$, 4: r/a about 0.5, 5: r/a about 0.25.

$r/a \approx 0.5$ suffer from higher losses (about 6 % of trapped plus passing particles) than reported in Lotz *et al.* (1992) (about 3 %).

To understand the possible reason for such a difference in particle losses, calculations of α-particle confinement for QHS are also performed for particles launched at positions with r/a somewhat smaller than 0.5.

As a result, particle losses of 3 % are found for starting positions at $r/a \approx 0.4$. For further analysis let us consider cross-sections of the magnetic surfaces for the considered QHS configuration which are shown in figure 4. Magnetic islands are seen in the near boundary region of the magnetic configuration. These islands correspond to resonant perturbations of the real-space magnetic field with $\iota = 3/2$. The formation of island magnetic surfaces instead of low-order rational surfaces, which are present in magnetic coordinates, leads to some deformation of adjacent non-island surfaces in the optimised VMEC equilibrium where particle losses have been minimised. Therefore, for some inner real space magnetic surfaces, which are not very far from the plasma boundary, the optimisation conditions will be somewhat violated. Due to

https://doi.org/10.1017/S0022377815001476 Published online by Cambridge University Press

this phenomenon, particle drift across magnetic surfaces as well as particle losses can be increased as compared to those found in magnetic coordinates and therefore the level of optimization may be reduced. Thus, the phenomenon related to the near boundary resonant-magnetic surfaces can be responsible for the higher level of particle losses at $r/a \approx 0.5$ in the real-space magnetic field as compared to those for the field given in the magnetic coordinates.

Note that the perturbation of the real-space magnetic field is a blend of resonant and non-resonant components. We focus on the analysis of the effect of the resonant component of the perturbation of the magnetic field, because the distortion of the magnetic field magnitude (obtained in magnetic coordinates) by the non-resonant magnetic field perturbation is proportional to the amplitude of this perturbation, while the distortion of this magnitude by the resonant magnetic field perturbation in regions adjacent to the resonant flux surface is proportional to the square root of the amplitude of the perturbation (see, e.g. Shaing 2002), i.e. is much greater than that for a non-resonant component. Configurations of Lotz *et al.* (1992), which are used for comparison with QHS, are somewhat different from the configuration of Nührenberg & Zille (1988). The configuration in Nührenberg & Zille (1988) has 6 field periods along the torus, whereas the configurations of Lotz *et al.* (1992) have 4 and 5 such periods. Besides that, the configuration with 4 field periods has a smaller aspect ratio than the configuration with 5 field periods. Nevertheless, the particle losses for these two configurations are the same. Therefore one can conclude that the level of particle losses calculated in magnetic coordinates for the configuration of Nührenberg & Zille (1988) will not be larger than that for the configurations in Lotz *et al.* (1992).

In conclusion, an attempt is made to reduce the sizes of the island at $\iota = 3/2$ by a change in the spectrum of the pertinent toroidal harmonic functions (set of 465 harmonics). These islands correspond to the presence of a harmonic with $m = 8$ and $n = -12$ in the spectrum (m is the poloidal number and n is the toroidal number, 8 islands are seen in the island chain in figure 4). One can try to reduce the sizes of the islands reducing the amplitude of this harmonic. It should be kept in mind that, in addition to the influence of the above mentioned harmonic on the resonance magnetic surface corresponding to $\iota = 3/2$, this harmonic also participates in the formation of the entire magnetic configuration and changing this harmonic can lead to destruction of a part of the configuration (since the decomposition coefficients for the initial harmonic set are obtained by satisfying the Neumann boundary condition at the VMEC boundary).

First, a case was considered when the harmonic $m = 8$, $n = -12$ is fully eliminated. It turned out that in such a case the magnetic surfaces are fully disrupted outside the surface corresponding to $r/a = 0.076$ (a is identified here with an average radius of the boundary surface, obtained with the aid of the VMEC code).

Since such a situation is unacceptable, a further study is performed where the amplitude of the $m = 8$, $n = -12$ harmonic is only slightly decreased. In figures 5 and 6 some results are presented for the case when the amplitude of this harmonic in the initial spectrum is decreased by 5 %. Figure 5 shows a cross-section of the magnetic surface by which the confinement region is now limited. Outside this surface magnetic surfaces are destroyed. It is seen that the confinement region now is noticeably smaller than in figure 4.

Calculations of the collisionless time evolution of the trapped α-particle fraction are carried out for a tracing time of 0.1 s. The results of calculations performed for particles started at $r/a \approx 0.25$ practically coincide with those in figure 3. However, for

https://doi.org/10.1017/S0022377815001476 Published online by Cambridge University Press

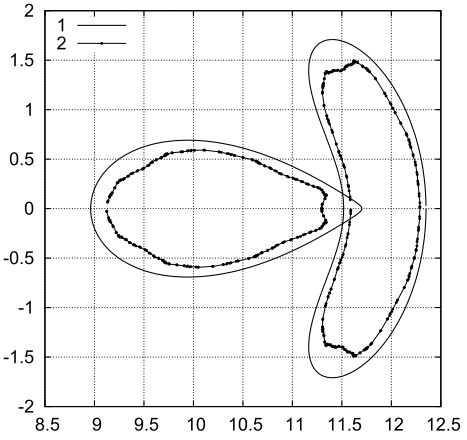

FIGURE 5. VMEC boundary (1) and outermos undestroyed magnetic surface for QHS with decreased amplitude of the resonant harmonic (2).

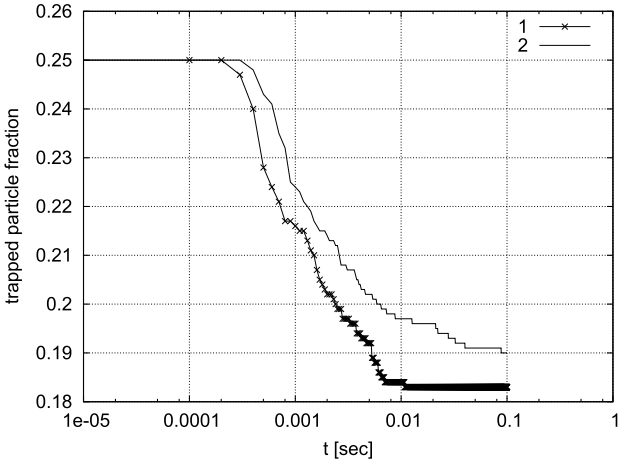

FIGURE 6. Collisionless evolution of the trapped α-particle fractions for QHS for decreased amplitude of the resonant harmonic (1). Particles are started on the magnetic surfaces corresponding to $r/a \approx 0.5$. Curve (2) shows the corresponding result from figure 3.

particles started at $r/a \approx 0.5$, the particle losses are now somewhat greater than those obtained before. The trapped particle evolution for this case is given in figure 6. The corresponding plot from figure 3 is also shown for comparison.

So, an attempt to suppress the islands near the boundary by some change of the harmonic spectrum led to a deterioration of the particle confinement. This can be understood from the difference between the modified spectrum and the spectrum obtain from VMEC using the Neumann boundary condition.

In addition to calculations with the set of 480 harmonics, calculations were also made for a set increased to 840 harmonics. For both sets, the results for the particle confinement turned out to be practically the same. In the calculations with the set of 840 harmonics, an attempt to suppress the influence of islands with $\iota = 3/2$ was

https://doi.org/10.1017/S0022377815001476 Published online by Cambridge University Press

undertaken, but now the fundamental harmonics of the spectrum are not changed. Instead of this, a small harmonic is added which is not contained in the fundamental spectrum, namely a harmonic $m = 8$, $n = -11$ or a harmonic $m = 8$, $n = -13$ with toroidal number close to $n = -12$. This is a multiple of the number of the field periods over the torus. The amplitude of the additional harmonic is set to 0.01 % of the amplitude of the fundamental harmonic $m = 8$, $n = -12$.

From the computational results it follows that in this case the magnetic surfaces are destroyed outside the surface corresponding to $r/a = 0.58$ ($n = -11$) or $r/a = 0.25$ ($n = -13$).

Note that in Nemov *et al.* (2014) a comparison has been carried out for the particle confinement in QHS with that in the HSX device (practical realization of the quasi-helically symmetric stellarator). There, the possibility of an improvement of particle confinement in the HSX has been discussed.

5. Conclusion

From the above results it follows that the appearance of magnetic islands differently affects the collisionless confinement of particles in magnetic configurations of standard and optimized stellarators. The standard stellarator configurations are less sensitive to the appearance of island magnetic surfaces than configurations of optimized stellarators. The computational results show that for U-2M and U-3M, the presence of island surfaces has practically no influence on collisionless α-particle confinement. However, particles started at a magnetic surface corresponding to approximately 0.5 of the minor radius in the real-space realisation of the quasi-helically symmetric stellarator (Nührenberg & Zille 1988) suffer from higher losses (6 %) as compared to those computed in magnetic coordinates (Lotz *et al.* 1992) (3 %). This difference can be attributed to the existence of magnetic islands in the near boundary region of the real-space magnetic field configuration. Of course, those islands are not present in the VMEC (Hirshman & Betancourt 1991) equilibrium, where only nested surfaces are possible. In a real space realisation, however, not only this rational surface is affected. The presence of islands leads to a deformation of adjacent non-island surfaces and thus the optimisation conditions are violated. This in turn leads to larger particle drift across magnetic surfaces and increased particle losses. Note that for the real-space realization of the QHS magnetic field, the harmonic spectrum is obtained using the Neumann boundary condition at the given VMEC boundary for the optimized configuration. Attempts to suppress the influence of the near boundary islands by changing this spectrum led to a reduction of the confinement region and deterioration of the particle confinement. This can be explained by violation of Neumann boundary condition at the VMEC boundary for the modified harmonic spectrum.

In summary, dedicated stellarator optimization clearly leads to a huge improvement in fast-particle confinement. Particle confinement studies, however, should not only rely on computations in magnetic coordinates.

Acknowledgements

This work has been carried out within the framework of the EUROfusion Consortium and has received funding from the Euratom Research and Training Programme 2014–2018 under grant agreement no. 633053. The views and opinions expressed herein do not necessarily reflect those of the European Commission.

REFERENCES

GRIEGER, G., LOTZ, W., MERKEL, P., NÜHRENBERG, J., SAPPER, J., STRUMBERGER, E., WOBIG, H., THE W7-X TEAM, BURHENN, R., ERCKMANN, V., GASPARINO, U., GIANNONE, L., HARTFUSS, H. J., JAENICKE, R., KÜHNER, G., RINGLER, H., WELLER, A., WAGNER, F. & W7-AS-TEAM 1992 Physics optimization of stellarators. *Phys. Fluids* B **4**, 2081–2091.

HIRSHMAN, S. P. & BETANCOURT, O. 1991 Preconditioned descent algorithm for rapid calculations of magnetohydrodynamic equilibria. *J. Comput. Phys.* **96**, 99–109.

LESNYAKOV, G. G., VOLKOV, E. D., GEORGIEVSKIJ, A. V., ZALKIND, V. M., KUZNETSOV, YU. K., OZHEREL'EV, F. I., PAVLICHENKO, O. S., POGOZHEV, D. P., SCHWÖRER, P. & HAILER, K. 1992 Study of the magnetic configuration of an $l=3$ torsatron by the triode and luminescent rod method. *Nucl. Fusion* **32**, 2157–2176.

LOTZ, W., MERKEL, P., NÜHRENBERG, J. & STRUMBERGER, E. 1992 Collisionless α-particle confinement in stellarators. *Plasma Phys. Control. Fusion* **34**, 1037–1052.

NEMOV, V. V., KASILOV, S. V. & KERNBICHLER, W. 2014 Collisionless high energy particle losses in optimized stellarators calculated in real-space coordinates. *Phys. Plasmas* **21**, 062501.

NÜHRENBERG, J. & ZILLE, R. 1988 Quasi-helically symmetric toroidal stellarators. *Phys. Lett.* A **129**, 113–117.

PAVLICHENKO, O. S. 1993 First results from the 'URAGAN-2M' torsatron. *Plasma Phys. Control. Fusion* **35**, B223–B230.

SHAING, K. C. 2002 Transport processes in the vicinity of a magnetic island in tokamaks. *Phys. Plasmas* **9**, 849–852.